# PROOF OF CONCEPT FOR AN INFRA-CIRCULATION FLUIDIC HIGH LIFT DEVICE

**Valeriu DRĂGAN**

INCDT Comoti, Bucharest, Romania,

***Abstract:*** *The paper refers to a new method for augmenting aerodynamic lift trough the use of fluidic jets acting as fluid barriers against the mainstream rather than the conventional boundary layer control jets in the current state of the art. Numerical simulations have been used to compare the proposed infra-circulation fluidic device with some of the most popular flaps configurations. In the matter of the lift to drag ratio and maximum lift coefficient, the proposed variation shows good comparative results especially at low angles of attack. Further development of the concept may yield efficient high lift devices for light aircraft and also for stealthier UAVs.*

***Keywords:*** *super circulation, high lift device, infra circulation, Coandă effect, flaps*

## 1. INTRODUCTION

State of the art fluidic high lift devices rely on the Coandă effect to either increase the circulation around the airfoil (super circulation) or to prevent or delay boundary layer separation (BLC) . As shown in many experimental Jones et al (2006), T.D. Economu & W.E. Milholen (2008), Buonanno (2009) and numerical studies Rumsey & Nishiro (2011), Guo et al. (2011), Dragan (2012), the fluidic methods are effective for a wide range of applications, including supersonic wings L. Robert & J.Englar (1975).

In theory, lift is linked to the circulation parameter Γ, trough the following relation

$$L=\rho\cdot\Gamma\cdot v \qquad (1)$$

It is therefore sensible to increase the circulation in order to achieve more lift. This, however, is not the only means to higher lift. This paper explores the possibility of using fluidic thin jets to perturb the mainstream in a controlled manner in order to locally decrease the static pressure on the top of the airfoil.

In V. Dragan & V.Stanciu(2012), a fluidic barrier is placed perpendicular to the mainstream, obstructing the flow locally and creating a positive pressure gradient in the underside of the airfoil.

Because the barrier is fluidic, rather than a solid surface, the drag that would be generated on a solid barrier is not transmitted to the airfoil, resulting in a high lift to drag ratio and also an increased maximum lift coefficient.

In this paper, a more radical approach is taken, by placing a cross flow jet near the leading edge on the upper side of the airfoil; a low pressure recirculation bubble is formed on the top of the airfoil leading to higher lift. It is clear that the concept is only applicable to very low angles of attack in order to avoid the increased induced drag (pressure drag) that would arise.

Figure 1 depicts the main differences between a fluidic barrier and a solid barrier placed at the same location on the airfoil.

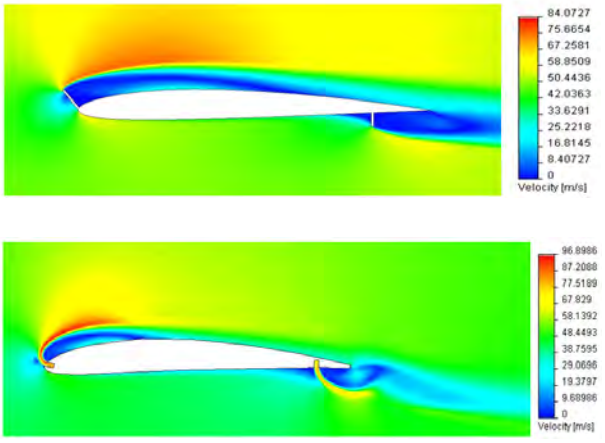


Fig. 1. Comparison between solid and fluidic barriers near the airfoil

Table 1. The forces acting upon the airfoil and the solid barriers

| Forces on Ox | [N] |
|---|---|
| Drag on airfoil | -25,2441 |
| Drag of underside barrier | 17,9225 |
| Drag of underside barrier | 56,5192 |
| **Total Drag** | **49,1976** |
| Forces on Oz | [N] |
| Lift on airfoil | 392,59 |
| Lift of underside barrier | -0,913544 |
| Lift of underside barrier | 46,5615 |
| **Total Lift** | **438,23796** |
| **Lift to Drag ratio** | **8,9077101** |

The proposed method sets itself apart from current fluidic high lift methods, introduces through his patents by Ion Stroescu (1925, 1927[a] and 1927[b]), synthesized in the lecture H. Dumitrescu (2010), in that it uses the jets not in order to control the boundary layer but to perturb the flow around the airfoil in a controlled manner. In other words, although the jets are thin and located in similar locations across the airfoil, the effect obtained – due to the blowing angle – is completely new.

## 2. THE COMPUTATIONAL STUDY

### 2.1 The case setup

For the numerical simulations, a k-epsilon realizable RANS model was used which is known to be more accurate in describing cross flows (Fluent™ User Guide). The mesh is two-dimensional and structured around a common sized airfoil chord of 1 m, which is placed in a stream at 50 m/sec. The test bed for this concept is a NACA 4410 airfoil with and without the fluidic spoiler (near the leading edge) and fluidic flaps (near the trailing edge). Multiple configurations of trailing edge and leading edge flaps have also been tested in order to compare their lift to drag ratio and wing loading with the ones obtained by the fluidic spoiler proposed herein.

By using a fluidic barrier, two effects contribute to the increased lift:

1. The increase of circulation around the airfoil due to the fluidic flaps (super circulation)

2. The decrease of the static pressure on the top of the airfoil due to the fluidic spoiler placed near the leading edge. The proposed term for this effect is infra-circulation, since the circulation near the recirculation bubble is lower than the one encountered under normal conditions.

An important note on the effect of the bubble near the leading edge is that the low pressure zone actually leads to an apparent thrust force (or, more appropriately, a negative drag component). This, however, should not be considered a gain (or erroneous result) since it is more than compensated by the thrust of the jet forming the barrier itself. For the calculation of the global lift to drag ratio, the following equation should be used:
For the fluidic spoiler

$$\frac{F_Z total}{F_X total} = \frac{F_Z + \sin\beta \cdot [A_{fantei} \cdot (P_{static} - P_{atm}) + \dot{m} \cdot u_j]}{F_X + \cos\beta \cdot [A_{fantei} \cdot (P_{static} - P_{atm}) + \dot{m} \cdot u_j]} \quad (2)$$

$A_{slot}$ = blowing slot surface area
$F_Z$ = lift of the airfoil surface
$F_X$ = drag of the airfoil surface
$P_{static}$ = static pressure of the jet
$P_{atm}$ = atmospheric pressure
$u_j$=blowing jet velocity
m = mass flow

Where $\beta$ is the sum of the angle of attack α and the angle of installation of the fluidic slot ζ,

$$\beta = \alpha + \zeta . \quad (3)$$

and for the fluidic flaps

$$\frac{F_Z total}{F_X total} = \frac{F_Z + \sin\alpha \cdot [A_{fantei} \cdot (P_{static} - P_{atm}) + \dot{m} \cdot u_j]}{F_X + \cos\alpha \cdot [A_{fantei} \cdot (P_{static} - P_{atm}) + \dot{m} \cdot u_j]} \quad (4)$$

In this particular case, we have chosen to use both fluidic systems in conjunction and, therefore, must use both equations to obtain correct interpretations of the results.

### 2.2 The fluidic jet barrier simulation

Two cases were studied; the first has the boundary conditions described in Table 2, the results in Table 3 and the flow field details illustrated in Fig. 2 and Fig. 3.

Table 2. Boundary conditions and global results for the fluidic barrier setup 1

| **Boundary conditions** | |
|---|---|
| Front jet velocity | 80 m/s |
| Low jet velocity | 75 m/s |
| Air speed | 50 m/s |
| **Results** | |
| Loading [Pa] | 1578,12921 |
| Lift to Drag | 75,0448675 |

Table 3. The defalcated force balance acting on the airfoil due to the fluid barrier influence

| $F_x$ | [N] |
|---|---|
| Drag | -18,7338 |
| Negative thrust of frontal fluidic jet | +22,4681 |
| **Total** | **+3,73** |
| $F_z$ | |
| Airfoil Lift | 264,259 |
| Negative Lift of frontal fluidic jet | -1,03 |
| Positive Lift of underside fluidic jet | +16,9 |
| **Total** | **280,2** |

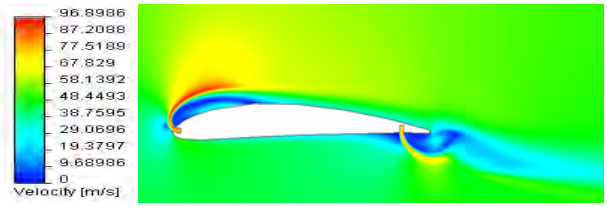


Fig. 2. Velocity flow field influenced by the two fluidic jets blowing against the mainstream

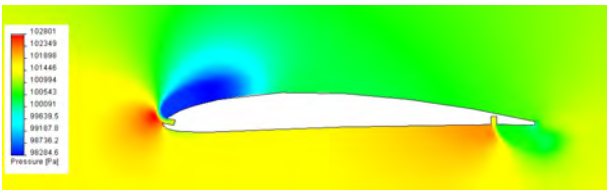

Fig. 3. Static pressure near the airfoil

Table 4. Boundary conditions and global results for the fluidic barrier setup 2

| **Boundary conditions** | |
|---|---|
| Front jet velocity | 100 m/s |
| Low jet velocity | 90 m/s |
| Air speed | 50 m/s |
| **Results** | |
| Loading [Pa] | 1885,4784 |
| Lift to Drag | 77,660152 |

Table 5. The defalcated force balance acting on the airfoil due to the fluid barrier influence

| $F_x$ | [N] |
|---|---|
| Drag | -24.45 |
| Negative thrust of frontal fluidic jet | +30,168776 |
| **Total** | +5,7187759 |
| $F_z$ | |
| Airfoil Lift | 264,259 |
| Negative Lift of frontal fluidic jet | -1,6204436 |
| Positive Lift of underside fluidic jet | +24,40258594 |
| **Total** | **370,15478** |

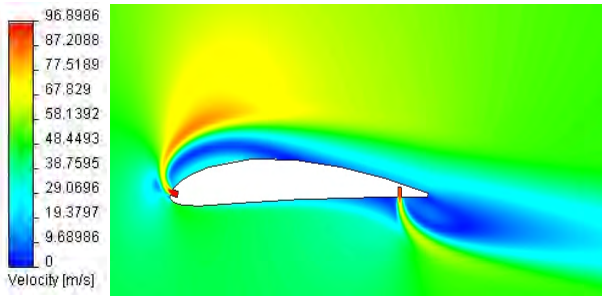


Fig. 4. The velocity flow field surrounding the airfoil.

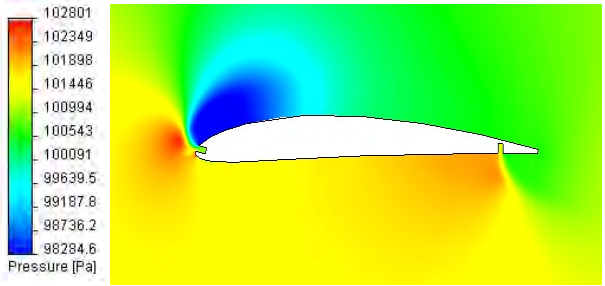


Note that the air forced to have a curved trajectory is accelerated, reminiscent of the Coandă effect.

Fig. 5. The low pressure bubble forming on the top of the airfoil as a result of the fluidic spoiler interaction with the mainstream

**2.3 Comparison with other know high lift devices**

In his paper, Smith (1975) presents the basic principles of multiple element airfoil theory. The paper presents the Handly-Page eight-element airfoil which, Smith concludes, is the limit to which multiple element airfoils can be designed efficiently.

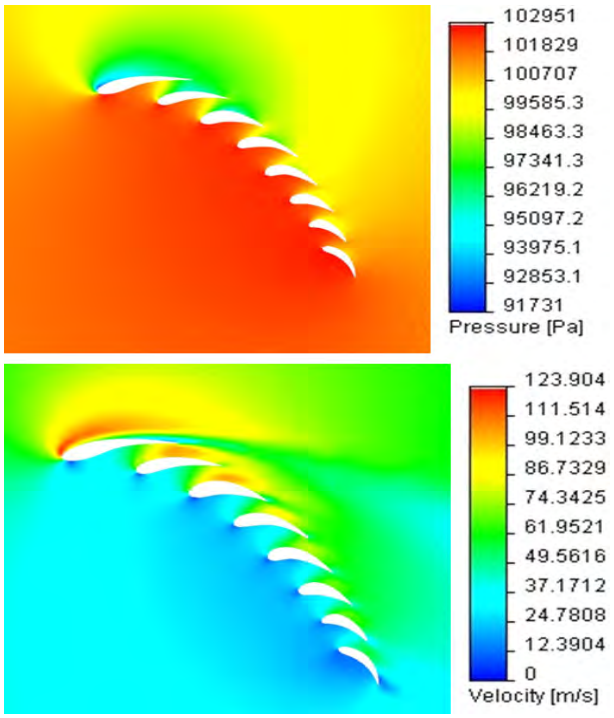


Fig.6. Handley-Page eight element airfoil Velocity and Static Pressure flow fields

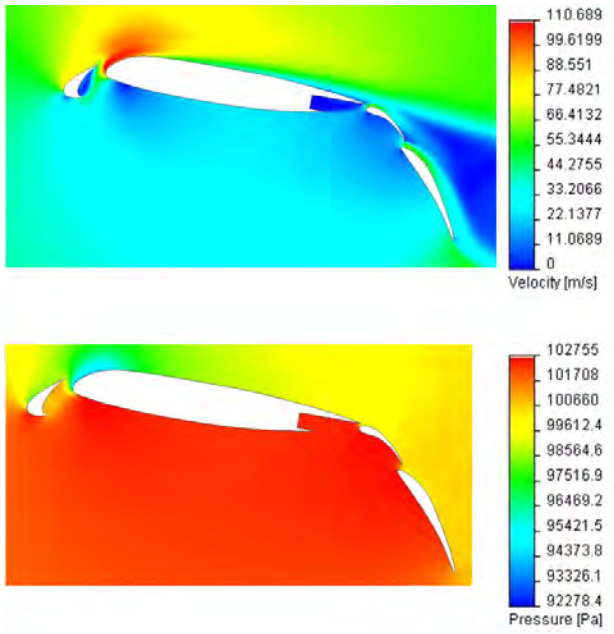


Fig. 7. Velocity and Static Pressure flow fields for 15º angle of attack of a bull-nose L.E. (Kruegger flap) + two slot T.E. flaps

In the User Manual of Zeusnumerix™ (2012), two more flaps configurations are discussed, the geometry was recreated and the same CFD methods applied in order to simulate the flow around them.

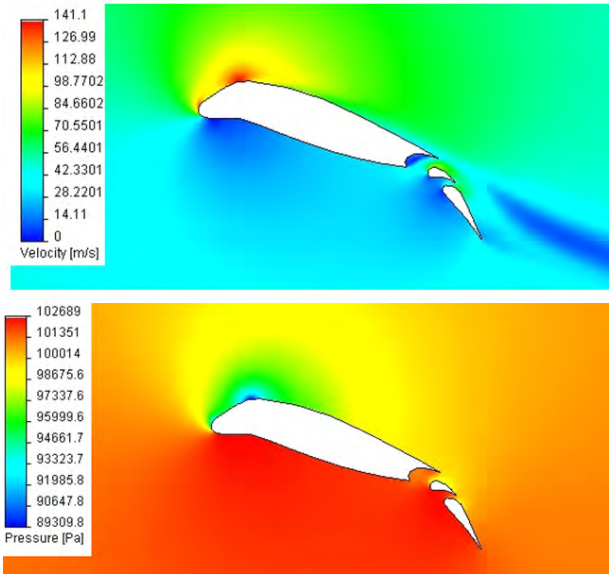


Fig. 8. Velocity and Static Pressure flow fields for the droop-L.E. + 2 slot T.E. configuration (adapted geometry from zeusnumerix).

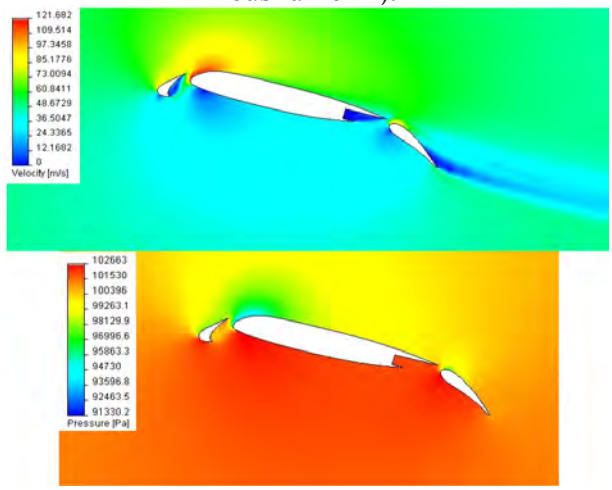

Fig. 9. The velocity magnitude flow field around the airfoil with single slot flaps and slat (adapted geometry from zeusnumerix)

From vanDam (2002), another geometrical configuration has been extracted and tested under the same conditions.

## 3. CONCLUSIONS

Through the use of a fluid barrier on the inner side and of a fluidic spoiler on the upper side of the test bed airfoil, higher wing loadings and increased lift to drag ratio are obtained. The charts below illustrate the differences between the baseline airfoil while comparing them with other commonly used high lift devices.

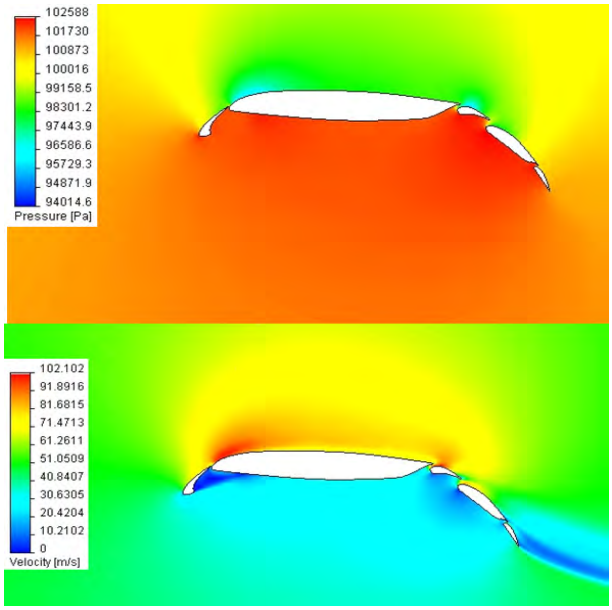


Fig. 10. Velocity and Static Pressure flow fields for the bull-nose L.E. and three slot T.E.

Two fluidic configurations have been used, having the physical parameters described in the tables in section 2. It is apparent that the velocity of the fluidic jets is a relevant factor since the amount of air entrained by them is directly influenced by the velocity magnitude. It has been observed that for a fluid barrier jet velocity of 1.5 times the free stream velocity, downstream of the airfoil there is no periodic vortex shedding. A possible explanation is that, at these values, the jet begins to behave similar to Spence's fluidic flaps which work on a completely different system in which the entrainment of air is more important than the local flow disturbances.

From Fig.1, which illustrates the velocity flow field, it is apparent that, due to the curvature of the streamlines, the fluid is accelerated as it passes the fluidic barrier. This behavior, explainable by the balance between the viscous, pressure and centrifugal forces is manifested both on the fluidic barrier and the fluidic spoiler. As such, a new facet of the Coandă effect may be studied, namely the Coandă effect on fluid surfaces. The two histograms below show that the use of both the fluidic spoiler and the fluidic barrier lead to higher section loadings and lift to drag ratios for the null angle of attack even in the case of an asymmetrical airfoil – such as the NACA 4410.

Possible applications of the principles described in this paper are aircraft which require a higher wing loading – and have a high landing speed – which can be reduced through the use of the fluid barriers. Also, stealthier high lift and/or maneuvering devices with no moving parts are potential applications of both the fluidic barrier and the fluidic spoiler presented here.

Table 6 – Synthesis of the CFD results

| Case | Loading [N/m$^2$] | L/D |
|---|---|---|
| NACA 4410 | 362.92278 | 17.455465 |
| NACA 4410 fluidic 1 AoA=0 | 1577.2984 | 75.044868 |
| NACA 4410 fluidic 2 AoA=0 | 1885.4784 | 77.660152 |
| Handley-Page | 3072.802 | 7.668583 |
| Kruegger 3 element flaps AoA=15 | 2851.662 | 7.061685 |

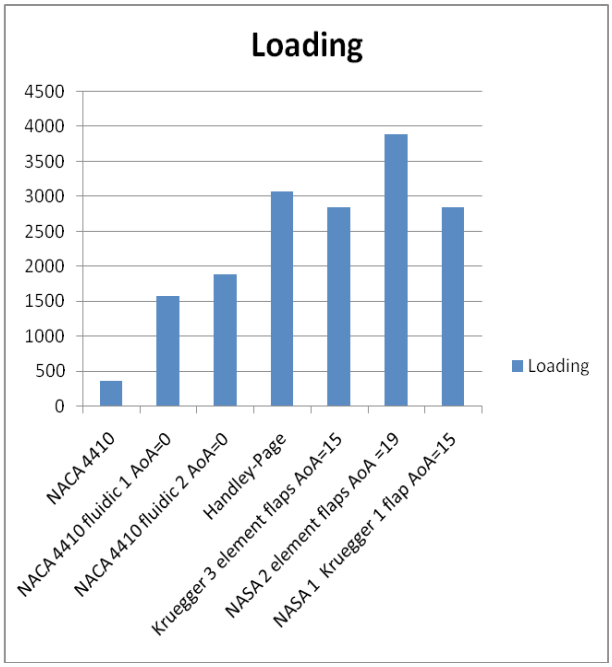


Fig. 11. Section loadings for the simulated high lift device configurations

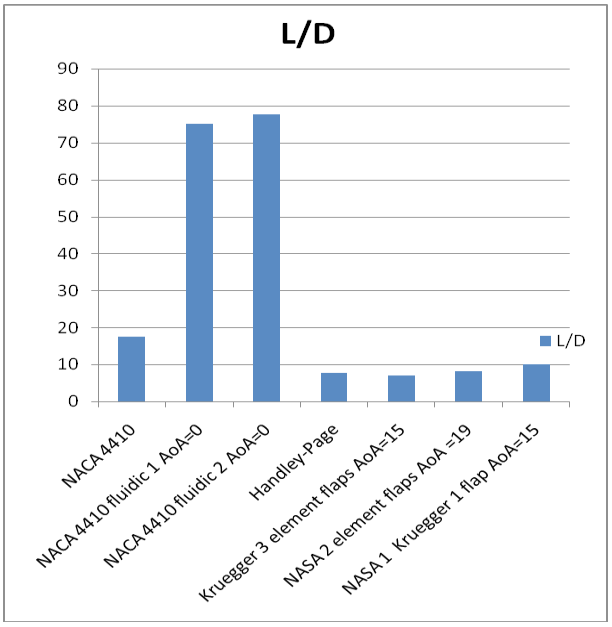


Fig. 12. Lift to Drag ratios for the simulated high lift device configurations

## REFERENCES


1. Ansys Fluent User Guide
2. Buonanno, Annalisa, Aerodynamic Circulation Control for Flapless Flight Control Of An Unmanned Air Vehicle, Cranfiel University. Ph.D. Thesis, 2009.
3. Dumitrescu Horia, „Professor Ion Stroescu and the boundary layer: a precursor of the flow control", INCAS Bulletin, Volume 3, Special Issue/ 2011, pp. 37-44, 2011.
4. Drăgan, Valeriu Aerodynamic and Acoustic Parameters of a Coanda Flow - a Numerical Investigation, Int. Transaction Journal of Engineering, Management, & Applied Sciences & Technologies, Vol 3, No. 1, 2012.
5. Drăgan, Valeriu Virgil Stanciu, Contributions regarding a fluid barrier supercirculation technique, UPB Scientific Bulletin D Series, 2013.
6. Economu, Thomas D. William E. Milholen II, Parametric Investigation of a 2-D Circulation Control Geometry, Stanford University Configuration Aerodynamics Branch Research and Technology Directorate Submitted, August 7, 2008.
7. Guo, B.D., Liu,P.Q., Qu,Q.L., Blowing Circulation Control on a Seaplane Airfoil, Recent progress in fluid dynamics research: Proceeding of the Sixth International Conference on Fluid Mechanics. AIP Conference Proceedings, Volume 1376, pp. 228-231, 2011.
8. Jones, Gregory, S. Chung-Sheng, Yao, Brian, G. Allan, Experimental Investigation of a 2D Supercritical Circulation-Control Airfoil Using Particle Image Velocimetry, AIAA 2006.
9. Smith, A. M. O. High-Lift Aerodynamics, VOL. 12, NO. 6, 37th Wright Brothers Lecture, Journal of Aircraft June 1975.
10. Spence, D.A., The Lift Coefficient of a Thin, Jet-Flapped Wing, Proceedings of the Royal Soc., Series A, Vol. 238, pp. 46-68.
11. Stroescu I. Romanian Patent nr. 11169 / 1925, „Aripă de avion cu țâșnitură de gaze". 1925
12. Stroescu I. Romanian Patent nr. 13676 / 1927, „Elice propulsoare cu jeturi fluide tangențiale". 1927
13. Stroescu I. Brevet nr. 13677 / 1927, „Dispozitiv pentru intensificarea sustentației prin metoda Lafay-Stroescu a jeturilor fluide tangențiale". 1927
14. Robert, L, Englar, J. Experimental investigation of the high velocity Coanda wall jet applied to bluff trailing edge circulation control airfoils. 1975
15. Rumsey, Nishiro, Numerical Study Comparing RANS and LES Approaches on a Circulation Control Airfoil, AIAA, 2011.
16. van Dam C.P., The aerodynamic design of multi-element high-lift systems for transport airplanes, Progress în Aerospace Sciences 38, pp. 101–144, 2002.
17. Zeusnumerix CFD Manual gallery